A&A 418, 655–661 (2004)
DOI: 10.1051/0004-6361:20040048

Astronomy & Astrophysics

BeppoSAX observations of the accretion-powered X-ray pulsar SMC X-1

S. Naik[1,2] and B. Paul[2]

[1] Department of Physics, University College Cork, Cork, Ireland
[2] Tata Institute of Fundamental Research, Homi Bhabha Road, Colaba, Mumbai, India

Received 27 May 2003 / Accepted 21 January 2004

Abstract. We present here results obtained from three *BeppoSAX* observations of the accretion-powered X-ray pulsar SMC X-1 carried out during the declining phases of its 40−60 days long super-orbital period. Timing analysis of the data clearly shows a continuing spin-up of the neutron star. Energy-resolved timing analysis shows that the pulse-profile of SMC X-1 is single peaked at energies less than 1.0 keV whereas an additional peak, the amplitude of which increases with energy within the MECS range, is present at higher energies. Broad-band pulse-phase-averaged spectroscopy of the *BeppoSAX* data, which is done for the first time since its discovery, shows that the energy spectrum in the 0.1−80 keV energy band has three components, a soft excess that can be modeled as a thermal black-body, a hard power-law component with a high-energy exponential cutoff and a narrow and weak iron emission line at 6.4 keV. Pulse-phase resolved spectroscopy indicates a pulsating nature of the soft spectral component, as seen in a few other binary X-ray pulsars, with a certain phase offset with respect to the hard power-law component. Dissimilar shape and phase of the soft and hard X-ray pulse profiles suggest a different origin of the soft and hard components.

Key words. stars: neutron – stars: pulsars: individual: SMC X-1 – X-rays: stars

1. Introduction

The bright, eclipsing, accretion-powered binary X-ray pulsar SMC X-1 was first detected during a rocket flight (Price et al. 1971). The discovery of X-ray eclipses with the *Uhuru* satellite established the binary nature of SMC X-1. The pulsar, with a pulse period of 0.71 s (Lucke et al. 1976), is orbiting a B0I super-giant (Sk 160) of mass ∼19 $M_{\odot}$ (Primini et al. 1977) with an orbital period of ∼3.89 days (Schreier et al. 1972). Since its discovery, observations with various X-ray observatories clearly show a steady spin-up of the neutron star in the binary system. This makes SMC X-1 an exceptional X-ray pulsar in which no spin-down episode has been observed (Wojdowski et al. 1998). An observed decay in the orbital period with a time scale of 3×10^6 yr (Levine et al. 1993) is interpreted as due to tidal interaction between the neutron star and the binary companion. The later is presumed to be in the hydrogen shell burning phase of its evolution. A super-orbital period of 40−60 days in SMC X-1, analogous to the well known X-ray pulsars Her X-1 and LMC X-4, was suggested by Gruber & Rothschild (1984) and was confirmed by recent observations with the *RXTE*/ASM and *CGRO*/BATSE (Clarkson et al. 2003). Varying obscuration by a precessing accretion disk provides a good explanation for the long term quasi-periodic intensity variations.

Send offprint requests to: S. Naik, e-mail: sachi@ucc.ie

Although the continuum energy spectrum of accreting X-ray pulsars is described by a power-law component with an exponential cutoff (White et al. 1983), there are some binary X-ray pulsars which show the presence of a soft excess over the extended hard power-law component. The soft component is detectable only in pulsars which do not suffer from absorption by material along the line of sight (Paul et al. 2002, and references therein). Pulsations in the soft spectral component with a certain phase difference with respect to the hard component are also seen in a few X-ray pulsars (Her X-1: Oosterbroek et al. 1997, 2000; Endo et al. 2000; SMC X-1: Paul et al. 2002; LMC X-4: Naik & Paul 2004). Apart from the hard and soft spectral components, iron emission line features are also seen in many of the X-ray pulsars. Iron K shell emission lines in X-ray pulsars are believed to be produced by illumination of neutral or partially ionized material in accretion disk, stellar wind of the high mass companion, material in the form of a circumstellar shell, material in the line of sight, or in the accretion column. Pulse-phase-averaged and pulse-phase-resolved spectroscopy, therefore, provide important information for understanding these systems in more detail.

The hard X-ray spectrum (20−80 keV energy band) of SMC X-1, obtained from the High Energy X-ray Experiment (*HEXE*) observations, was fitted with a thin thermal bremsstrahlung spectrum with a plasma temperature of ∼14.5 keV (Kunz et al. 1993). Though a pure power law

spectrum was rejected, a power law component modified with an exponential cutoff also provided a good fit to the *HEXE* data. The broad-band X-ray spectrum (0.2−37 keV) of SMC X-1 was earlier studied by fitting combined spectra obtained from the *ROSAT* and *Ginga* observations (Woo et al. 1995). The energy spectrum is best fitted with a model consisting of a cutoff power-law type component, soft excess which is modeled as a single blackbody component, and a broad iron emission line. Pulsating hard X-rays and non-pulsating soft X-rays were detected from observations made with *HEAO* 1 A-2 and *Einstein* SSS (Marshall et al. 1983). However, pulse-timing analysis of the *ROSAT* and *ASCA* observations shows clear pulsations of the soft X-rays with a pulse profile different to that of the hard component (Wojdowski et al. 1998). Pulse-phase-resolved spectroscopy of *ASCA* data in the 0.5−10.0 keV energy band shows a pulsating nature of the soft component with some phase difference compared to the hard X-rays (Paul et al. 2002) as is seen in some other binary X-ray pulsars. The nearly sinusoidal single peaked profile of the pulsating soft component contrasts with the double peaked profile seen at higher energies. As the *ASCA* GIS spectrometers are not sensitive at energies where the soft excess dominates (<0.6 keV), it is interesting to probe the nature of the soft spectral component over the pulse period of the 0.7 s pulsar in SMC X-1 with the *BeppoSAX* LECS.

In this paper, we present the broad band X-ray spectrum of SMC X-1 over three decades in energy. We have carried out detailed timing and spectral analysis of three observations of SMC X-1 with the Low Energy Concentrator Spectrometers (LECS), Medium Energy Concentrator Spectrometers (MECS) and the hard X-ray Phoswich Detection System (PDS) instruments of *BeppoSAX* in the energy band of 0.1−80.0 keV during the decaying state of the 40−60 days super-orbital period of SMC X-1. To examine the nature of the soft excess, pulse-phase-resolved spectral analysis has been carried out for the observation with highest X-ray intensity. In the subsequent sections we give details of the observations, the results obtained from the timing and spectral analysis, followed by a discussion on the results obtained from these three *BeppoSAX* observations.

2. Observations

The long term periodic intensity variation of SMC X-1, which was discovered with the instruments on *HEAO-I* (Gruber & Rothschild 1984), is clearly seen in the *RXTE*-ASM light curve. The *RXTE*/ASM light curve of the source, from 1996 December to 1997 June (50420−50620 MJD range) is shown in Fig. 1. The observations of SMC X-1 which were made with the *BeppoSAX* instruments during 1997 January 14 17:26 to 23:55 UT (with 7, 20.5, and 7.5 ks useful exposures for LECS, MECS and PDS respectively), 1997 March 02 07:14 to 14:30 UT (with 7.5, 21.5 and 7 ks useful exposure) and 1997 April 25 16:38 to 23:12 UT (with 7.5, 21.5 and 8.5 ks useful exposure) in the high states of the 40−60 days quasi-periodic super-orbital period, are marked in the figure. All three *BeppoSAX* observations were made in the orbital phase 0.40−0.54 with the estimated mid-eclipse times taken as phase zero. We have used the archival data from these observations to study the timing and spectral behavior of the source.

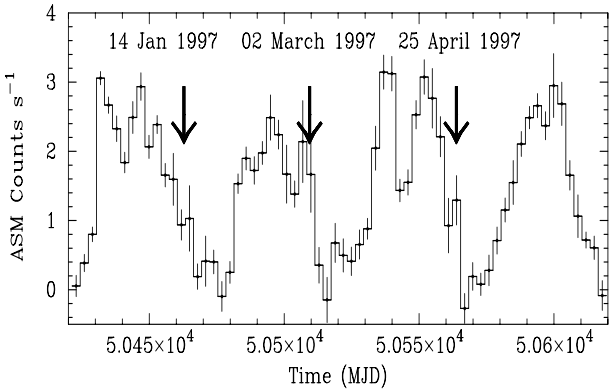

Fig. 1. The RXTE-ASM light curve of SMC X-1 from 1996 December 03 (MJD 50 420) to 1997 June 21 (MJD 50 620). The arrows mark the dates of the *BeppoSAX* observations which are used for the analysis.

For the present study, we have used data from the LECS, MECS and PDS instruments on-board *BeppoSAX* satellite. The MECS consists of two grazing incidence telescopes with imaging gas scintillation proportional counters in their focal planes. The LECS uses an identical concentrator system as the MECS, but utilizes an ultra-thin entrance window and a driftless configuration to extend the low-energy response to 0.1 keV. The PDS detector is composed of 4 actively shielded NaI(Tl)/CsI(Na) phoswich scintillators with a total geometric area of 795 cm^2 and a field of view of 1.3° (*FWHM*). Time resolution of the instruments during these observations was 15.25 μs and energy resolutions of LECS, MECS, and PDS are 25% at 0.6 keV, 8% at 6 keV and ≤15% at 60 keV respectively. For a detailed description of the *BeppoSAX* mission, we refer to Boella et al. (1997) and Frontera et al. (1997).

3. Timing analysis

Data from LECS, MECS, and PDS detectors were used for timing analysis. The arrival times of the photons were first converted to the same at the solar system barycenter. Light curves with time resolution of 7 ms were extracted from circular regions of radius 4′ around the source. To detect the pulsations during these observations, the light curves were first corrected for the arrival time delays due to orbital motion. The semi-amplitude of the orbital motion was taken to be 53.4876 ls and the mid-eclipse time was derived from the quadratic solution given by Wojdowski et al. (1998). After the barycenter correction and correction due to the orbital motion, pulse folding and a χ^2 maximization technique was applied for pulsation analysis. We have derived the pulse periods of SMC X-1 to be 0.70722816(8) s, 0.70718014(4) s and 0.7071143(7) s on 1997 January 14, 1997 March 02 and 1997 April 25 respectively. The pulse periods obtained from these three *BeppoSAX* observations and those obtained from previous studies (given in Table 1) are plotted against time and shown in Fig. 2 along with a fitted quadratic function of time (upper panel) and the deviations from the fit (bottom panel). The coefficients

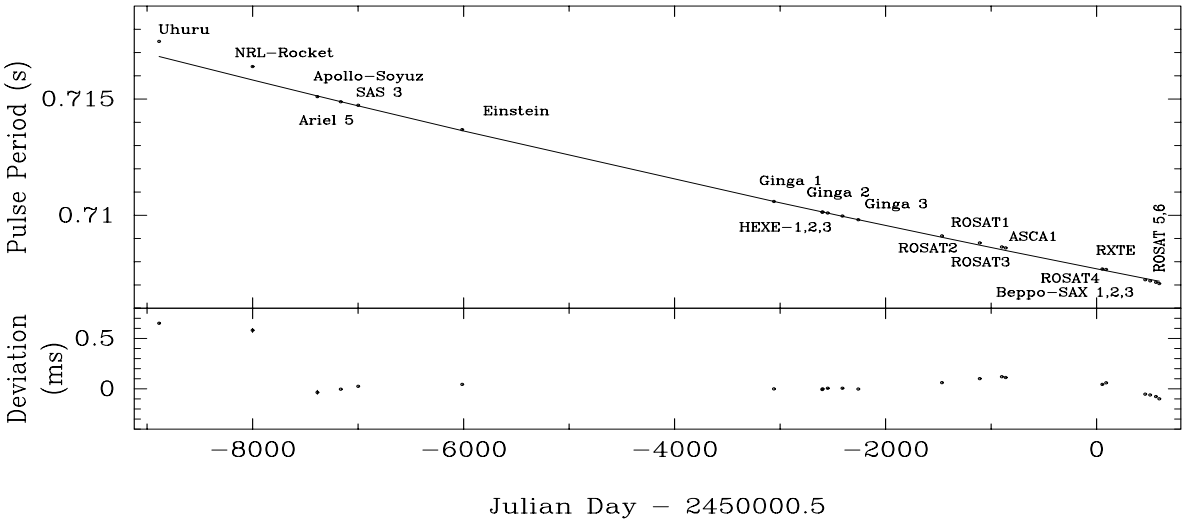

Fig. 2. Pulse periods of SMC X-1 obtained from 1997 *BeppoSAX* observations along with those obtained from previous studies are plotted against time together with a fitted quadratic function (*top panel*) and the deviations from the fit (*bottom panel*).

Table 1. Summary of pulse period measurements of SMC X-1 used in present work other than that reported in Wojdowski et al. (1998).

Observatory	Pulse period (s)	Epoch (MJD)	Ref.
HEXE-1	0.7101362(15)	47 399.5	1
HEXE-2	0.7100978(15)	47 451.5	1
HEXE-3	0.7099636(15)	47 591.0	1
BeppoSAX-1	0.7072282(81)	50 460.9	2
BeppoSAX-2	0.7071801(44)	50 507.6	2
BeppoSAX-3	0.7071144(71)	50 562.1	2
ROSAT-4	0.70769(6)	50 054.0	3
ROSAT-5	0.707065(10)	50 593.8	3
ROSAT-6	0.706707(10)	50 898.2	3

1: Kunz et al. (1993); 2: present work; 3: Kahabka & Li (1999).

Table 2. Coefficient of the quadratic fit to the pulse period data of SMC X-1.

Parameter[1]	Value
p_0	0.7076955 s
p_1	-9.05×10^{-7} s day^{-1}
p_2	1.38×10^{-11} s day^{-2}
t_0	2 450 000.5 JD

$P_{\rm pulse} = p_0 + p_1(t - t_0) + p_2(t - t_0)^2$.

obtained from the quadratic fit to the pulse periods are listed in Table 2. It is observed that, since discovery, the neutron star in the SMC X-1 binary system follows a spin-up trend without any spin-down episode.

The pulse profiles in different energy bands obtained from the LECS, MECS, and PDS light curves from the 1997 March 02 observation are shown in Fig. 3. In the low energy band (0.1−1.0 keV of LECS, top panel), the pulse profile is nearly sinusoidal and single peaked. However, an additional peak appears in the pulse profiles at higher energies as shown in the second, third, fourth, and fifth panels of Fig. 3. The amplitude of the second peak increases with energy and is comparable with that of the main peak as seen in the 4.0−10.0 keV pulse profile (bottom panel of Fig. 3). The light curve above 30 keV is mainly background dominated and clear pulsations are not detected in the 30−60 keV energy band.

4. Spectral analysis

4.1. Pulse phase averaged spectroscopy

For spectral analysis, we have extracted LECS spectra from regions of radius 6′ centered on the object (the object was at the center of the field of view of the instrument). The combined MECS source counts (MECS 1+2+3) were extracted from circular regions with a 4′ radius. The September 1997 LECS and MECS1 response matrices were used for the spectral fitting. Background spectra for both LECS and MECS instruments were extracted from the appropriate blank fields with regions similar to the source extraction regions. We rebinned the LECS, MECS and PDS spectra to allow the use of the χ^2-statistic. Events were selected in the energy ranges 0.1−4.0 keV for LECS, 1.65−10.0 keV for MECS and 15.0−80.0 keV for PDS where the instrument responses are well determined. The combined spectra from the LECS, MECS and PDS detectors, after appropriate background subtraction, were fitted simultaneously. All the spectral parameters other than the relative normalization were tied to be the same for all the three detectors and the minimum value of hydrogen column density $N_{\rm H}$ was set at the value of the Galactic column density in the source direction.

The broad-band energy spectrum (0.1−80 keV) of SMC X-1, when simultaneously fitted to a single power-law model with line of sight absorption, showed the presence of an iron emission line at 6.4 keV and a significant amount of soft excess at low energies (<1 keV). Paul et al. (2002) found that the soft excess detected with *ASCA* spectrometers can be fitted with different model components such as blackbody emission, bremsstrahlung-type thermal component, a soft

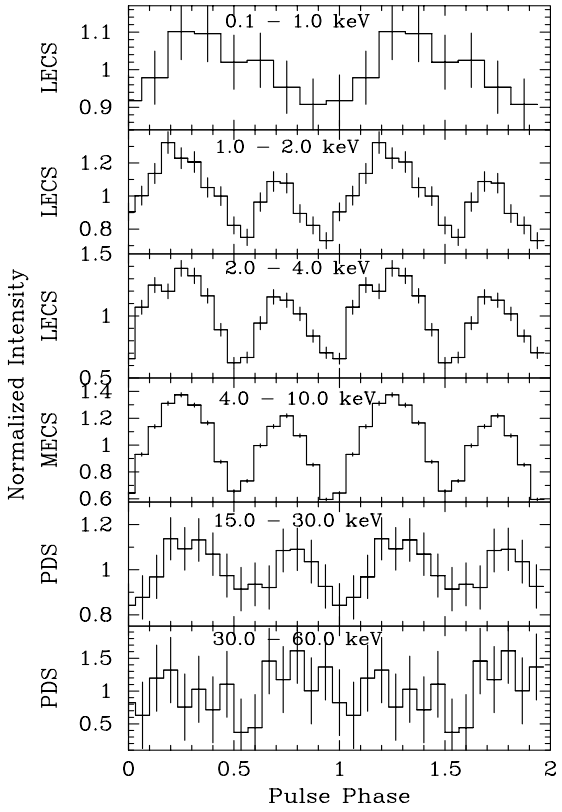

Fig. 3. The LECS, MECS, and PDS pulse profiles of SMC X-1 during the high state of the 40−60 days super-orbital period (1997 March 02 *BeppoSAX* observation) are shown here for different energy bands with 8 phase bins (*top panel*) and 16 phase bins (*other panels*) per pulse. Two pulses in each panel are shown for clarity.

Table 3. Spectral parameters for SMC X-1 during 1997 *BeppoSAX* observations.

Parameter	14 January	02 March	25 April
Model-I (Wabs * (bb + po + Ga) * highecut)			
$N_{\rm H}^1$	$3.41^{+0.13}_{-0.46}$	2.55 ± 0.09	$2.11^{+1.43}_{-0.84}$
Γ	0.86 ± 0.02	0.82 ± 0.02	0.77 ± 0.01
kT (keV)	0.16 ± 0.01	0.19 ± 0.01	0.19 ± 0.01
$E_{\rm c}$ (keV)	6.43 ± 0.11	6.30 ± 0.09	6.41 ± 0.13
$E_{\rm f}$ (keV)	$11.03^{+0.27}_{-0.15}$	10.58 ± 0.13	$10.14^{+0.29}_{-0.16}$
W_0 (eV)	25	15	19
Total flux[2]	4.5×10^{-10}	5.0×10^{-10}	3.1×10^{-10}
BB flux[3]	1.8×10^{-11}	2.2×10^{-11}	1.1×10^{-11}
Line flux[4]	1.4×10^{-12}	0.9×10^{-12}	0.7×10^{-12}
Reduced χ^2	1.2 (176)	1.2 (168)	0.98 (167)
Model-II (Wabs * (bb + comptt + Ga))			
$N_{\rm H}^1$	$1.06^{+0.42}_{-0.31}$	$1.17^{+0.39}_{-0.40}$	$0.53^{+0.17}_{-0.11}$
kT (keV)	$0.29^{+0.03}_{-0.03}$	$0.29^{+0.03}_{-0.02}$	$0.34^{+0.03}_{-0.04}$
T_0 (keV)	$0.81^{+0.07}_{-0.08}$	$0.95^{+0.12}_{-0.06}$	$0.94^{+0.08}_{-0.08}$
kT_e (keV)	$5.43^{+0.21}_{-0.10}$	$5.93^{+0.19}_{-0.18}$	$5.34^{+0.16}_{-0.22}$
τ	$6.47^{+0.10}_{-0.23}$	$6.09^{+0.19}_{-0.34}$	$6.44^{+0.21}_{-0.22}$
Reduced χ^2	1.3 (169)	1.3 (169)	1.1 (169)

Γ = power-law photon index; $E_{\rm c}$ = cutoff energy; $E_{\rm f}$ = e-folding energy; W_0 = iron equivalent width.
[1] 10^{21} atoms cm^{-2}; [2] flux in 0.1−10.0 keV energy band in ergs cm^{-2} s^{-1}; [3] blackbody flux in ergs cm^{-2} s^{-1}; [4] iron line flux in ergs cm^{-2} s^{-1}.

power-law, or an inversely broken power-law. Simultaneous spectral fitting to the LECS, MECS and PDS spectra shows that the hard power-law component has an exponential cutoff at ∼6 keV, as was found by Woo et al. (1996), with an e-folding energy of ∼11 keV. With the *BeppoSAX* combined spectrum, we found that addition of a blackbody emission component for the soft excess and a Gaussian function at 6.4 keV for the iron K$_\alpha$ emission line with the hard power-law continuum model fits the spectra well.

The analytical form of the model used for spectral fitting to the 0.1−80.0 keV band energy spectrum is
Model-I:

$$f(E) = {\rm e}^{-\sigma(E)\ N_{\rm H}}[f_{\rm bb}(E) + f_{\rm pl}(E) f_{\rm cut} + f_{\rm Fe}(E)]$$

where E is the energy of the incident photon and $\sigma(E)$ is the photoelectric absorption cross section and

$$f_{\rm bb}(E) = \frac{I_{\rm bb}(E/kT_{\rm bb})^2(e-1)}{{\rm e}^{E/kT_{\rm bb}} - 1},\ \ f_{\rm pl}(E) = I_{\rm pl}\ E^{-\Gamma},$$

$$f_{\rm Fe}(E) = \frac{I_{\rm Fe}}{\sqrt{2\pi\sigma_{\rm Fe}^2}} \exp\left[-\frac{(E - E_{\rm Fe})^2}{2\sigma_{\rm Fe}^2}\right]$$

$$f_{\rm cut} = \begin{cases} 1, & E < E_{\rm c} \\ {\rm e}^{-(E-E_{\rm c})/E_{\rm f}}, & E \geq E_{\rm c}. \end{cases}$$

In all three *BeppoSAX* observations, the power-law photon index is found to be ∼0.8, and the hydrogen column density along the line of sight ($N_{\rm H}$) is in the range of 2.1−3.4 × 10^{21} atoms cm^{-2}. The blackbody component, of temperature 0.16−0.19 keV, dominates the spectrum at energies below 1.0 keV. The iron K$_\alpha$ emission line, centered at 6.4 keV, is found to be very weak during all the observations with very low equivalent width. Since the iron line center energy is very close to the power-law cut-off energy, the presence of the former was separately verified by fixing the continuum model based on data outside the 5.5−7.5 keV range. Assuming a distance of 65 kpc to SMC X-1, we have estimated the X-ray luminosity L_x in the 0.1−80 keV energy band to be 5.8×10^{38} erg s^{-1}, 6.9×10^{38} erg s^{-1}, and 4.6×10^{38} erg s^{-1} for the observations on 1997 January 14, March 02, and April 25 respectively. The spectral parameters and the reduced χ^2 for all the *BeppoSAX* observations of SMC X-1 made in 1997 are given in Table 3. From the spectral fitting, it can be seen that all the fitted parameters are identical for these three *BeppoSAX* observations. The LECS, MECS and PDS count rate spectra of 1997 March 02 *BeppoSAX* observation are shown in Fig. 4 along with contributions of individual components in top panel, whereas the residuals to the best-fit model are shown in the bottom panel.

We have also tried to fit the LECS, MECS, and PDS spectra with a model consisting of a blackbody emission component for the soft excess and the Comptonization continuum component (implemented as of "*comptt*" in

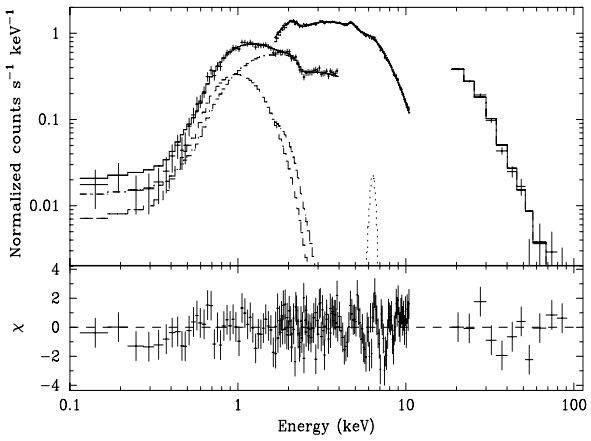

Fig. 4. Energy spectra of SMC X-1, during the high intensity state of the 40−60 days long super-orbital period, obtained with the LECS, MECS and PDS detectors of the 1997 March 02 observation, along with the best-fit model comprising soft blackbody emission, narrow iron line emission, and a cutoff power-law component. The bottom panel shows the contributions of the residuals to the χ^2 for each energy bin.

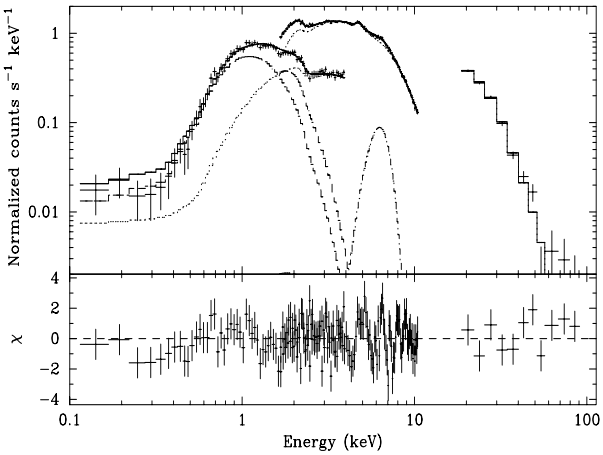

Fig. 5. Same as Fig. 4, but with the Comptonization continuum model.

XSPEC package) of Titarchuk (1994) as was done for GX 1+4 and RX J0812.4−3114 by Galloway et al. (2001). The addition of a Gaussian function though improves the spectral fitting, it gives an unusual emission line, centered around 5.2−5.7 keV, and a high blackbody temperature of about ∼2 keV. We have, therefore, fixed the iron line energy at 6.4 keV and allowed the width and normalization to vary. The spectral parameters of the CompTT model thus obtained are also given in Table 3. The count rate spectra of the 1997 March 02 observation are shown in the upper panel of Fig. 5 along with the residuals to the best-fit Comptonization model in the bottom panel. It can be seen that the soft spectral component dominates the energy spectrum up to ∼2 keV. Therefore, in this model, we expect that the pulse profiles in the energy band of 0.1−2.0 keV should be identical. However, the pulse profiles in the 0.1−1.0 keV and 1.0−2.0 keV energy bands, as shown in Fig. 3, are quite different and the reduced χ^2 obtained for the Comptonization model is also larger compared to the power-law model in all three observations. We therefore conclude that the SMC X-1 spectrum is best described as an exponential cutoff power-law with blackbody emission (for soft excess) and iron emission line.

We checked the bremsstrahlung model (Kunz et al. 1993) by fitting the *BeppoSAX* PDS spectrum of the 1997 March observation in the 15−80 keV energy band. The plasma temperature obtained from spectral fitting is found to be 15 keV with a reduced χ^2 of 1.7 for 55 degrees of freedom. However, the broad-band *BeppoSAX* spectrum with LECS, MECS, and PDS data, when fitted simultaneously with the thermal bremsstrahlung model along with a blackbody emission component for soft excess and an iron K_α line, gives a very poor fit with a reduced χ^2 of 13.6 for 172 degrees of freedom.

4.2. Pulse phase resolved spectroscopy

All the observations of SMC X-1 with the *BeppoSAX* were made near the edge of the high state of the 40−60 day super-orbital period (Fig. 1) and within 0.4−0.54 orbital phase. For pulse phase resolved spectroscopy, we have chosen the *BeppoSAX* observation made on 1997 March 02 when the source count rate was higher compared to the other two observations. The data from the LECS and MECS detectors are used for pulse-phase-resolved spectroscopy as we aimed at the study of the nature of the soft spectral component in SMC X-1.

Following barycenter and arrival time corrections to the LECS and MECS event files, spectra were accumulated into 16 pulse phases by applying phase filtering in the FTOOLS task XSELECT. As in the case of phase-averaged spectroscopy, the background spectra were extracted from source-free regions in the event files, and appropriate response files were used for the spectral fitting. The phase-resolved spectra were fitted with a model consisting of a high energy cutoff power-law component along with the blackbody emission for soft excess and iron K_α emission line. The iron-line energy, line-width and $N_{\rm H}$ were fixed to their phase-averaged values and all the other spectral parameters were allowed to vary. The continuum flux and the fluxes of the soft and hard components in the 0.1−10.0 keV energy range were estimated for all the 16 phase-resolved spectra. The modulation in the X-ray flux for the hard and soft spectral components and the total flux are shown in Fig. 6 along with the 1σ error estimates. Pulse-phase-resolved spectral analysis shows that modulation of the hard power-law flux is very similar to the pulse profile at higher energies. The soft spectral component is identical in shape with what was obtained with the *ASCA* (Paul et al. 2002). The short duration of the *BeppoSAX* observation, however, has resulted into relatively large error bars, and a nonvarying soft excess cannot be ruled out from this data.

5. Discussion

5.1. Pulse period evolution of SMC X-1

Accurate pulse period measurement of a number of X-ray pulsars has been achieved over the last three decades using various

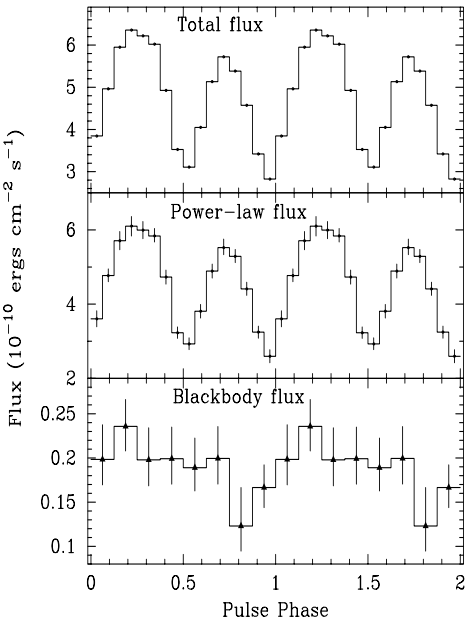

Fig. 6. Modulation of the total flux, hard power-law flux and flux of the soft spectral component in 0.1−10.0 keV energy band of SMC X-1 obtained from the pulse-phase-resolved spectroscopy of the LECS and MECS spectra obtained from 1997 March 02 *BeppoSAX* observation. The lower panel is rebinned to 8 bins.

X-ray observatories (Bildsten et al. 1997). X-ray pulsars which accrete matter from the stellar wind of the companion star often show irregular spin rate changes on longer time scales, whereas the disk accreting pulsars generally show long-term systematic changes in spin period. On the shortest time scales, however, the change in spin period appears to be comparable in both groups of X-ray pulsars.

In the standard accretion-disk model, a pulsar can spin at an equilibrium period if the spin-up torque given by the accreting matter is balanced by a braking torque due to the interaction of the magnetic field with the accretion disk outside the corotation radius (Ghosh & Lamb 1979). For a neutron star with given magnetic moment, the equilibrium spin period depends on the accretion rate, and the pulsar is expected to spin-up or down as the accretion rate increases or decreases. The observed correlations between the pulse period and the luminosity of X-ray pulsars establish the consistency of the model. Using hydromagnetic equations, Ghosh & Lamb (1979) calculated the torque on the neutron star and found that for sufficiently high stellar angular velocities or sufficiently low mass accretion rates the rotation of the star can be braked while accretion continues.

The observed mean spin-up rate in the SMC X-1 system makes it unique among the close binary systems with supergiant companion in which mass accretion takes place from the stellar wind. The period evolution of SMC X-1 is quite different from other persistent HMXB pulsars. *BATSE* observations (Bildsten et al. 1997) showed that accreting pulsars with massive companions (eg. Cen X-3) show short term spin-up and spin-down episodes. Though Cen X-3 shows 10−100 day intervals of steady spin-up and spin-down trend at a much larger rate, it also shows a long term spin-up trend which is the average of the frequent transition between spin-up and spin-down episodes (Finger et al. 1994). In SMC X-1, however, the absence of spin-down (torque reversal) episodes in more than three decades makes it different from other pulsars which show a long term spin-up trend. The monotonous decrease in the derived pulse period of SMC X-1 with time suggests that the accretion flow has never slowed enough to allow any breaking in the neutron star rotation, and that SMC X-1 is far from an equilibrium rotator. It can be noted that considering the low metallicity of the SMC/LMC, the wind of the supergiant companions alone cannot account for the large persistent X-ray luminosities of the pulsars like SMC X-1 and LMC X-4. Roche Lobe overflow as a partial accretion mechanism is a distinct possibility in these binary systems, which is also probable in Cen X-3.

5.2. Broad band X-ray spectrum of SMC X-1

Since the detection of X-ray emission from SMC in 1971, the accretion powered high mass X-ray binary pulsar SMC X-1 has been observed with many different X-ray observatories. Though the pulse phase averaged spectral studies of SMC X-1 have been done in different energy bands using X-ray data from various instruments such as 20−80 keV from *HEXE* observations (Kunz et al. 1993), 0.2−37 keV from *ROSAT* and *Ginga* observations (Woo et al. 1995), 0.1−10 keV from *Chandra* observations (Vrtilek et al. 2001), 0.5−10 keV from *ASCA* observations (Paul et al. 2002), a broad band X-ray spectral study in the 0.1−80 keV energy range is reported for the first time here. A thermal bremsstrahlung model, used to describe the 20−80 keV hard X-ray spectrum (Kunz et al. 1993) is ruled out while fitting the source spectrum in 0.1−80 keV energy range. A Comptonization continuum component, used to describe the spectrum of a few other accretion powered X-ray pulsars, is also found to be unsuitable for spectral fitting in comparison to the hard power-law continuum component. Simultaneous spectral fitting to the broad band X-ray spectrum of the source, therefore, shows significant improvement in understanding the accretion processes in the binary system.

Broad-band pulse-phase-averaged spectroscopy of SMC X-1 shows the presence of a weak and narrow iron emission line with very low equivalent width (∼20 eV), and soft excess above the hard power-law continuum component as seen in several accreting pulsars. A detailed and systematic analysis of X-ray spectra of SMC X-1 at different phases of its 40−60 days super-orbital period would establish the spectral variations of the source over the third period. A correlation between the hard X-ray continuum flux and the iron emission line flux, and the highly variable nature of the otherwise constant iron equivalent width during the low intensity states have been found in other X-ray binary pulsars with super-orbital period (LMC X-4 and Her X-1, Naik & Paul 2003).

5.3. Nature of the soft excess

Accreting X-ray binary pulsars which do not suffer from strong absorption by the material along the line of sight show soft excess over the hard power-law component. Her X-1

(Endo et al. 2000), SMC X-1 (Paul et al. 2002), EXO 053109−6609.2 (Haberl et al. 2003; Paul et al. 2004), and LMC X-4 (Naik & Paul 2004) are the sources in which the difference in the pulse profiles in the soft and hard X-ray bands along with the presence of a soft component over the dominating hard power-law component have already been reported. Some of the sources also show pulsations in the soft component. The pulsating nature of the soft blackbody component with a certain phase difference compared to the hard component and heterogeneous pulse profiles at different energy bands suggest a different origin of emission of the soft and hard components. Endo et al. (2000) discussed the origin of the soft and hard spectral components in Her X-1 and suggested that the hard power-law component originates from the magnetic poles of the neutron star in the binary system whereas the origin of the soft blackbody component is believed to be the inner edge of the accretion disk. A blackbody or thermal bremsstrahlung type emission component fits the soft excess of SMC X-1 and LMC X-4 (Paul et al. 2002). However, from *BeppoSAX* observations of LMC X-4 in the high state, Naik & Paul (2004) have established a pulsating nature of the soft component which rules out the bremsstrahlung model.

The soft spectral component derived from the *BeppoSAX* observations is entirely compatible with the results from the *ASCA* spectra (Paul et al. 2002). However, a short exposure of only 7.5 ks with the LECS during this SAX observation does not allow us to determine accurately the shape and phase of the soft component. Therefore, from the present observation we cannot rule out a nonvarying soft excess.

Acknowledgements. We thank an anonymous referee for her/his valuable suggestions which improved the content of this paper. We thank Dr. P. J. Callanan for a careful reading of the paper. The *BeppoSAX* satellite is a joint Italian and Dutch program. We thank the staff members of *BeppoSAX* Science Data Center and RXTE/ASM group for making the data public.

References

Bildsten, L., Chakrabarty, D., Chiu, J., et al. 1997, ApJS, 113, 367
Boella, G., Butler, R. C., Perola, G. C., et al. 1997, A&AS, 122, 299
Clarkson, W. I., Charles, P. A., Coe, M. J., et al. 2003, MNRAS, 339, 447
Endo, T., Nagase, F., & Mihara, T. 2000, PASJ, 52, 223
Finger, M. H., Wilson, R. B., & Fishman, G. J. 1994, in Second Compton Symposium, ed. C. E. Fichtel, N. Gehrels, & J. P. Norris (New York: AIP), 304
Frontera, F., Costa, E., Dal Fiume, D., et al. 1997, A&AS, 122, 357
Galloway, D. K., Giles, A. B., Wu, K., & Greenhill, J. G. 2001, MNRAS, 325, 419
Ghosh, P., & Lamb, F. K. 1979, ApJ, 234, 296
Gruber, D. E., & Rothschild, R. E. 1984, ApJ, 283, 546
Haberl, F., Dennerl, K., & Pietsch, W. 2003, A&A, 406, 471
Kahabka, P., & Li, X.-D. 1999, A&A, 345, 117
Kunz, M., Gruber, D. E., Kendziorra, E., et al. 1993, A&A, 268, 116
Levine, A., Rappaport, S., Deeter, J. E., et al. 1993, ApJ, 410, 328
Lucke, R., Yentis, D., Friedman, H., et al. 1976, ApJ, 206, L25
Marshall, F. E., Becker, R. H., & White, N. E. 1983, ApJ, 266, 814
Naik, S., & Paul, B. 2003, A&A, 401, 265
Naik, S., & Paul, B. 2004, ApJ, 600, 351
Oosterbroek, T., Parmar, A. N., Martin, D. D. E., & Lammers, U. 1997, A&A, 327, 215
Oosterbroek, T., Parmar, A. N., Dal Fiume, D., et al. 2000, A&A, 353, 575
Paul, B., Nagase, F., Endo, T., et al. 2002, ApJ, 579, 411
Paul, B., Jaaffery, S. N., Naik, S., & Agrawal, P. C. 2004, ApJ, 602, 913
Price, R. E., Groves, D. J., Rodrigues, R. M., et al. 1971, ApJ, 168, L7
Primini, F., Rappaport, S., & Joss, P. C. 1977, ApJ, 217, 543
Schreier, E., Giacconi, R., Gursky, H., et al. 1972, ApJ, 178, 71
Titarchuk, L. 1994, ApJ, 434, 570
Vrtilek, S. D., Raymond, J. C., Boroson, B., et al. 2001, ApJ, 563, L139
White, N. E., Swank, J. H., & Holt, S. S. 1983, ApJ, 270, 711
Wojdowski, P., Clark, G. W., Levine, A. M., et al. 1998, ApJ, 502, 253
Woo, J. W., Clark, G. W., Blondin, J. M., et al. 1995, ApJ, 445, 896
Woo, J. W., Clark, G. W., Levine, A. M., et al. 1996, ApJ, 467, 811